

## Numerical Simulations of the Ambipolar Filamentation Process

M. Franqueira

*Dept. Astronomía y Geodesia, Fac. CC. Matemáticas,  
 Universidad Complutense de Madrid, Avda. Complutense s/n,  
 E-28040 Madrid, Spain*

M. Tagger

*CEA Saclay, Service d'Astrophysique, DSM/DAPNIA/Sap,  
 F-91191 Gif-sur-Yvette, France*

A.I. Gómez de Castro

*Dept. Astronomía y Geodesia, Fac. CC. Matemáticas,  
 Universidad Complutense de Madrid, Avda. Complutense s/n,  
 E-28040 Madrid, Spain*

### Abstract.

We are carrying out 2-D, two-fluid (ions and neutrals) numerical simulations of the ambipolar filamentation process, in which a magnetized, weakly ionized plasma is stirred by turbulence in the ambipolar frequency range. The higher turbulent velocity of the neutrals in the most ionized regions gives rise to a non-linear force driving them out of these regions, so that the initial ionization inhomogeneities are strongly amplified. This effect, the ambipolar filamentation, causes the ions and the magnetic flux to condense and separate from the neutrals, resulting in a filamentary structure. This mechanism might help to explain some problems arising in magnetized and partially ionized astrophysical plasmas. It might provide an explanation for the spicules emerging from the solar photosphere. We also expect it to have an important role in star formation. Under molecular cloud conditions (supersonic turbulence), we expect the mechanism to result in an additional pressure from the most ionized to the least ionized regions that efficiently separates the ions from the neutrals, favoring the gravitational collapse of the latter.

*Keywords:* ISM: Ambipolar Diffusion, Turbulence, Ionization, Filaments, Gravitational Collapse; Stars: Formation

### 1. The Ambipolar Filamentation

Magnetic fields contribute to the dynamical behavior of ionized astrophysical fluids such as those in the upper solar and stellar atmospheres, the interstellar medium and star-forming regions. Their influence is carried out by hydromagnetic waves which efficiently propagate perturbations. However, Kulsrud & Pearce (1969) showed that in the magnetized and weakly ionized interstellar medium hydromagnetic waves are heavily damped since they do not propagate

in a frequency range (and thus scale) associated with ambipolar diffusion (the *ambipolar range*, between the ion-neutral and neutral-ion collision frequencies  $\nu_{in}$  and  $\nu_{ni}$ ) where the neutrals are imperfectly coupled to the ions and the waves are strongly damped by ion-neutral friction.

We are interested in the non-linear evolution of this process, which can cause the *ambipolar filamentation* of the magnetic field (Tagger, Falgarone & Shukurov 1995) as follows: when a magnetized and weakly ionized plasma that shows small variations in the ionization fraction ( $Z = \rho_i/\rho_n$ ) is stirred by hydromagnetic turbulence in the ambipolar range, the turbulent velocity of the neutrals is higher in the most ionized regions, since they are better coupled to the ions. This gives rise to a force (given by the average of the  $v \cdot \nabla v$  term) driving the neutrals out of the most ionized regions. By reaction the ions and magnetic flux are compressed in these regions, so that the initial ionization inhomogeneities are strongly amplified. This is expected to result in a condensation of the flux tubes, producing a filamentary structure.

## 2. The Numerical Code

In order to study the efficiency of this non-linear mechanism we simulated its behavior numerically. The full set of magnetohydrodynamics (MHD) equations describing a two-fluid (ions and neutrals) system, given by Langer (1978), must be solved. Our numerical code solves the simplified two-dimensional problem (in  $y$ -horizontal and  $z$ -vertical directions): all quantities are  $x$ -invariant, so only the perturbed current has a component along  $x$ , which is taken into account.

Our code is based on the same general methods as the ZEUS-2D code (Stone & Norman 1992). It solves the MHD equations on a staggered mesh using the method of finite differences with a time explicit, multistep (operator split) scheme (see Franqueira, Tagger & Gómez de Castro 2000 for a complete description of the numerical code).

The boundary conditions are periodic in the  $y$  direction. At  $z = 0$  we launch an Alfvén wave by giving the whole fluid (neutrals, ions and magnetic field lines) a motion in  $y$  which, in this first numerical test of the mechanism, is limited to a single periodic oscillation ( $v_y(y, 0) = v_t \cos(\omega t)$ ). This will propagate upward as an Alfvén wave. At the opposite boundary ( $z_{max}$ ) we impose reflective boundary conditions; they have no real effect since the total length in  $z$  is chosen such that the waves are heavily damped before they reach that point.

In order to isolate the effect we want to study, we impose that there is no flux of matter from  $z = 0$  into the simulation box. This is the most severe constraint on the code because the wave pressure pushes matter upward, resulting in very low densities at the first grid points.

## 3. The Simulations

We follow the evolution of a 2-D, two fluid system (ions and neutrals) with low ionization fraction. The gas is initially threaded by a vertical constant magnetic

field and perturbed by horizontal Alfvén waves excited at the footpoints of the magnetic field lines ( $z = 0$ ).

We assume initial equilibrium in a fluid vertically stratified and supported by gravity, with ions and neutrals densities decreasing sharply (by a factor  $\sim 10$ ) with  $z$  (Fig. 1). Initially the neutral density is independent of  $y$ , but the ion density shows a small enhancement in the  $y$  direction. The magnetic field is adjusted so as to ensure MHD equilibrium in the  $y$  direction, given by  $\frac{\partial}{\partial y} \left( p_i + \frac{B^2}{8\pi} \right) = 0$ . The resulting initial ionization fraction  $Z_0$  is constant over  $z$  but shows a maximum at  $y = 0$  (Fig. 2).

The frequency of the wave is chosen so that it propagates without damping at the lower part of the simulation grid ( $\omega \ll \nu_{ni}$ ), but is strongly damped at intermediate altitudes, where  $\rho_i$  (and thus  $\nu_{ni}$ ) was taken to decrease sharply. Therefore the filamentation will occur only at the intermediate altitude where the wave is damped (Tagger et al. 1995) but still retains a strong perturbed velocity. In the simulation presented, the perturbed velocity of the wave at  $z = 0$  is of the order of the sound velocity ( $v_t = 0.7c_s$ ), which is taken to be half the Alfvén velocity.

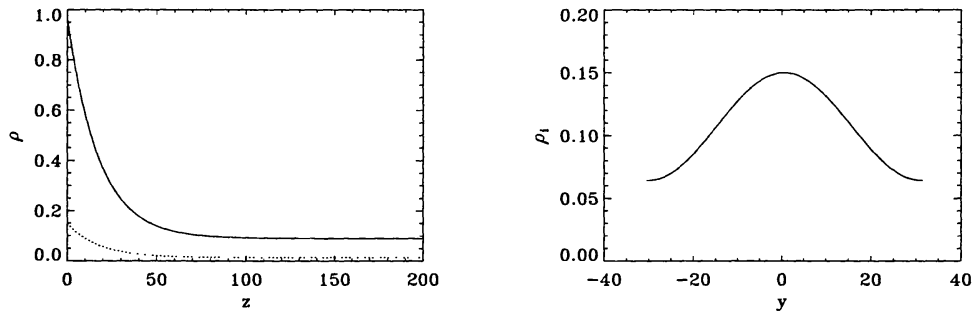


Figure 1. Left: Initial ions (dotted line) and neutrals (solid line) density profiles in the  $z$  direction at  $y = 0$ . Right: Initial ions density profile in the  $y$  direction at  $z = 0$ . We have normalized the parameters to the characteristic scales of the problem we are solving. Therefore we have taken as units the initial Alfvén velocity at  $z = 0$ ,  $v_A$ , and the Alfvén time  $t_A$ , defined as the time that takes such an Alfvén wave in crossing one wavelength  $\lambda_A$ . We use the grid zone indices to scale the horizontal ( $y$ ) and vertical ( $z$ ) directions in all figures.

#### 4. Results

We find a strong amplification (by a factor  $\sim 2.5$ ) of the contrast in  $Z$  (Figs. 2 and 3), at the altitude where the wave is damped (Fig. 3). At the same altitude the  $\rho_i$  contrast along  $y$  grows and the most ionized region shrinks, as expected (Fig. 4 left). Moreover the ion density decreases on the sides of the peak, suggesting ion motion towards the most ionized regions. The neutrals are expelled

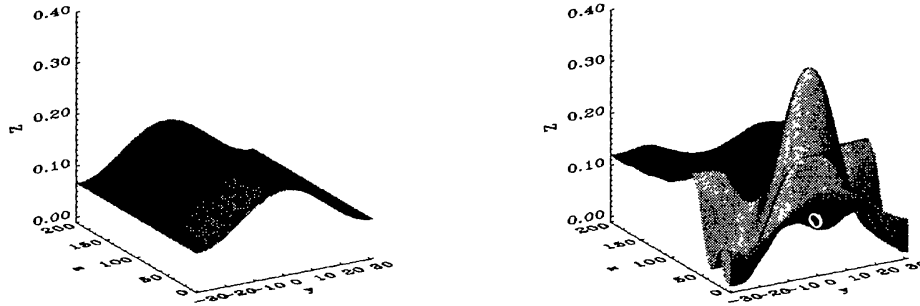


Figure 2. Left: Initial 2D distribution of the ionization fraction  $Z = \rho_i/\rho_n$  in the calculation grid. Right: Spatial profile of the ionization fraction after  $6.7 \times 10^3$  Alfvén times. The initial contrast in the horizontal direction has grown and shrunk at the altitude where the wave is damped.

from the most ionized regions (Fig. 4 right), generating in the density profile a “central” minimum of the same order as the increase achieved by the ions.

The condensation of the ions must be accompanied by a compression of the magnetic field lines, but numerical resistivity allows the field to diffuse almost totally. A small residual amplification of the central field lines is left but it is undetectable at low altitudes, where the wave dominates the field dynamics. However, at the highest grid zones, where the wave is almost completely damped, the increase in  $B$  can be barely detected. It causes the rise of the magnetic pressure, which results in an expulsion of ions from the central field lines at high altitudes, so that a reversed ion density profile appears (Fig.2 right).

For the lowest values of the perturbed velocity ( $v_t$ ) a state of equilibrium is achieved early in the calculation (Fig.5). However, for the highest velocities the filamentation is more efficient and causes the simulation to crash. The asymptotic value of  $Z_{max}$  varies quadratically with  $v_t$ , as expected from the theory (Tagger et al. 1995).

## 5. Applications

The ambipolar filamentation mechanism might help to explain the fibrilled structure observed in the magnetic field emerging from the solar photosphere; in particular we consider an explanation for the spicules. We expect our mechanism to act together with the vertical flow of matter discussed in Haerendel (1992), Tagger et al. (1995) and De Pontieu & Haerendel (1998). Upward traveling Alfvén waves generated in the photosphere are expected to cause both ambipolar filamentation of the field lines (expelling the neutrals from the most ionized flux tubes, thus concentrating the magnetic flux in narrow tubes) and vertical acceleration of the gas.

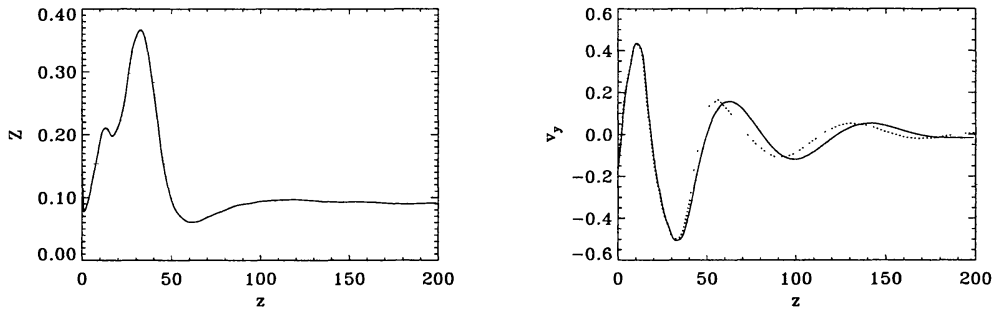


Figure 3. Left: Vertical profile of the ionization fraction  $Z$ . Right: Vertical profile of the transverse perturbed velocities of ions (solid) and neutrals (dotted). The decoupling of the two fluids begins at the altitude where the wave is damped and a phase lag appears.

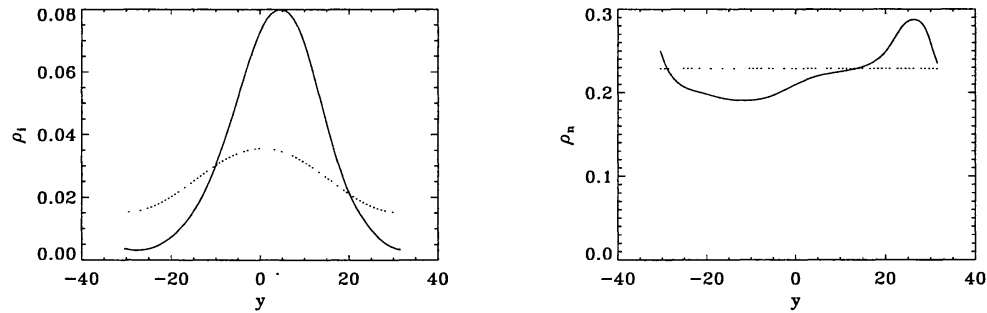


Figure 4. Ions density (left) and neutrals density (right) profiles in  $y$  direction at the altitude where the ionization fraction  $Z$  reaches its maximum. Dotted lines show the initial values. The minimum/maximum are not centered at  $y = 0$  because of the lateral motion due to the wave.

Models of star formation (since the early work of Arons & Max 1975) invoke molecular clouds supported essentially by turbulent magnetic pressure and an ambipolar flow of the neutrals toward dense cores (Arons & Max 1975; Shu et al. 1987; McKee et al. 1993; Vázquez-Semadeni et al. 2000; and references therein). In molecular clouds, where turbulence is supersonic, we expect our mechanism to result in an additional pressure from the most ionized to the least ionized regions that efficiently separates the ions from the neutrals, favoring the gravitational collapse of the latter.

Another subject for future work could be the strong spatial and temporal intermittency of MHD turbulence. This is known to occur in intense current and vorticity sheets (see Spangler 1999, and references therein; Falgarone 1999 and Falgarone & Phillips 1990). We can expect our mechanism to be particularly efficient in those sheets where gradients of all quantities become strong on extremely small scales, and where turbulent motions concentrate.

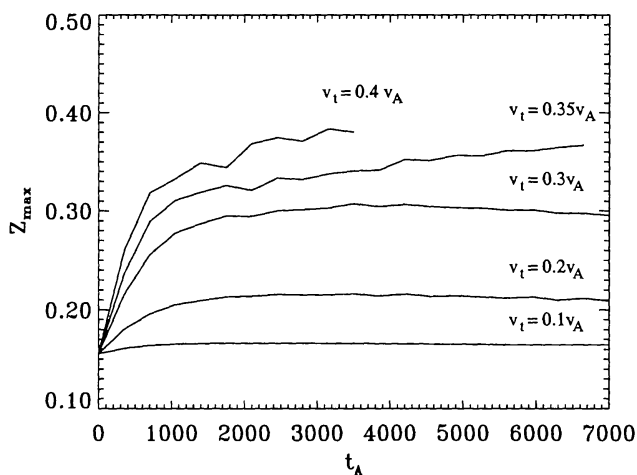


Figure 5. Time evolution of the value of maximum ionization fraction for different initial perturbed velocities.

## References

- Arons, J. & Max, C.E. 1975, *ApJ lett.*, 196, L77  
 De Pontieu, B. & Haerendel, G. 1998, *A&A*, 338, 729  
 Falgarone, E. 1999 in *Interstellar Turbulence*, ed. J. Franco, & A. Carramiñana (Cambridge University Press) 132  
 Falgarone, E. & Phillips, T.G. 1990, *ApJ*, 359, 344  
 Franqueira, M., Tagger, M. & Gómez de Castro, A.I. 2000, *A&A*, 357, 1143  
 Haerendel, G. 1992, *Nat*, 360, 241  
 Kulsrud, R. & Pearce, W. 1969, *ApJ*, 156, 445  
 Langer, W.D. 1978, *ApJ*, 225, 95  
 McKee, C.F., Zweibel, E.G., Goodman, A.A. & Heiles, C. 1993 in *Protostars and Planets III*, E.H. Levy, J.I. Lunine (Tucson: University of Arizona press), 327  
 Shu, F.H., Adams, F.C. & Lizano, S. 1987, *ARA&A*, 25, 23  
 Spangler, S.R. 1999, *ApJ*, 522, 879  
 Stone, J.M. & Norman, M.L. 1992a, *ApJS*, 80, 753  
 Tagger, M., Falgarone, E. & Shukurov, A. 1995, *A&A*, 299, 940  
 Vázquez-Semadeni, E., Ostriker, E.C., Passot, T., Gammie, C.F. & Stone, J.M. 2000 in *Protostars and Planets IV*, ed. V. Mannings, A. Boss, & S. Russell (Tucson: University of Arizona press), 1

### 3. Collapse and protostars

